Krzysztof Okoń, Anna Sińczak-Kuta

Nuclear Morphometry as a Tool of Limited Capacity for Distinguishing Renal Oncocytoma from Chromophobe Carcinoma

Department of Pathomorphology, Jagiellonian University, Collegium Medicum

The principal types of renal tumors include malignant clear cell renal cell carcinoma, chromophobe carcinoma (ChRCC), papillary carcinoma and benign oncocytoma (RO) and adenoma. Both oncocytoma and chromophobe carcinoma are characterized by a solid growth pattern of cell with abundant cytoplasm and in some cases may be difficult to distinguish based on histology only. The material for the study consisted of 58 chromophobe carcinomas and 16 oncocytomas. At least 100 nuclei per case were segmented from images of DAPI-stained slides. The geometric and texture features were extracted and used for analysis. Significant differences between RO and ChRCC were found in all the analyzed parameters, however overlapping of the features exists. None of the constructed models permitted to classify cases in concordance with diagnoses.

Introduction

Renal cell tumors, especially carcinoma, are increasing in frequency according to most studies [6]. This increase was estimated to equal 2% per year [19]. The main categories of renal tumors are conventional (clear cell) carcinoma, chromophobe renal cell carcinoma (ChRCC), collecting duct carcinoma and papillary carcinoma; commonly seen benign tumors include renal oncocytoma (RO) and adenoma [6, 7, 17, 18]. The distinction between chromophobe renal cell carcinoma and oncocytoma may be difficult in some cases. Differential diagnosis of renal cell tumors will also become extremely important when specific treatment modalities will be introduced [9].

The aim of the present study was to test the performance of image analysis-based approach to distinguishing chromophobe RCC from oncocytoma.

Material and Methods

The material consisted of 74 cases (58 ChRCC and 16 RO) found among 775 renal tumors diagnosed in our institution between 1992 and 2005. The material was formalin-fixed, routinely processed and paraffin-embedded. From the tissue blocks, 3μm sections were prepared and stained with hematoxilin-eosin. Cases with extensive necrosis, cystic tumors with tiny foci of neoplastic epithelium and secondary tumors were excluded from consideration. All the cases were reclassified according to the WHO system [6]. The reclassification was based on HE slides, with the use of Hale colloid iron, PTAH, paS staining and immunohistochemistry for epithelial membrane antigen, pan-cytokeratin, cytokeratins 7, 19, 20, 34βE12, CD10, HMB-45 when appropriate. For the purpose of the study, chromophobe carcinoma (ChRCC) was defined as a tumor composed of cells with abundant, lightly eosinophilic cytoplasm with clear 'halo' around nucleus, submembranous CK7 staining and Hale colloid iron positive. Oncocytoma (RO) was defined as composed of oncocytic regular cells with negative colloid iron staining. For immunohistochemistry, the standard staining protocol was used. Briefly, the slides were dewaxed, rehydrated and incubated in 3% peroxide solution for 10 minutes to block endogenous peroxidase activity. Antigen retrieval was carried out by microwaving in citrate buffer (0.2% citric acid titrated to pH 6.0 with 2N NaOH)

for 3x5 minutes at 750 W. Primary antibodies against EMA (clone E29, DAKO, Denmark, diluted to 1:100), panCK (clone MNF116, DAKO, diluted to 1:50), CK7 (clone OV-TL12/30, DAKO, Denmark, diluted to 1:50), CK19 (clone RCK108, DAKO, diluted to 1:50), CK20 (clone Ks20.8, DAKO, diluted to 1:50), CD10 (clone 56C, Novocastra Ltd, UK, diluted to 1:50), vimentin (clone V9, DAKO, diluted 1:50), HMB-45 (clone HMB-45, DAKO, diluted 1:50) were used. The ENVISION (DAKO, Denmark) detection system was employed. 3-amino-9-ethylcarbasole (DAKO, Denmark) was used as the chromogen. The slides were counterstained with Mayer hematoxilin (DAKO, Denmark). All the tumors were restaged by the newer AJCC and traditional Robson systems.

Hematoxilin-eosin sections were reviewed and in each case, a section was selected that would contain a representative and well-preserved carcinoma. Slides for image analysis were stained with 1000ng/ml DAPI solution and examined under a fluorescence microscope. The system of image acquisition and analysis consisted of an Axioscop microscope (Zeiss, Germany) with a 100W HBO mercury lamp and a 100x Plan-NeoFluar immersing lens, a CCD ZVS-47DE camera (Optronics, USA) connected by a RGB line with the GraBIT PCI card (Soft Imaging System GmbH, Germany) of a standard PC running the Windows XP Professional (Microsoft Corp., USA) operating system. The custom-made software was developed in the Imaging C (ANSI C) language and was running in the AnalySIS v. 3.2 pro (Soft Imaging System GmbH, Germany) image analysis environment [23]. For each case, 20 to 30 images were recorded in the TIFF format. The files contained information about the case identity. In the subsequent step, the images were read from the disk, filtered, segmented with an automatic threshold setting, and accurately segmented nuclear profiles were selected by the operator. Individual nuclei were again saved in the TIFF format. The procedure was continued until at least 100 nuclei per case were acquired. In the next phase, geometric and textural features of the nuclei were extracted in batch processing mode, and the results were saved in a text file.

The term "texture" refers to the fashion, in which smaller patterns are arranged on a surface. There are several methods of quantifying texture properties [14, 15, 20]. The simplest one is to measure the grey level standard deviation or variance. Their high values may indicate a greater variation of pixels in the image. Other methods commonly used for texture evaluation are grey level correlation matrix and Laws matrix derived energy. Apart from regional distribution of chromatin, its central or peripheral location within the nucleus is also important. For this purpose, central moments invariants [13, 21] were used. All the textural measurements were done both on raw and histogram-equalized images. Table 1 summarizes the parameters used.

For statistical analysis, the χ^2 test, Kruskall-Wallis ANOVA, one way, multidimensional and nested ANOVA were used if appropriate. Clustering and classification was

TABLE 1
Nuclear features used in the investigation.

geometric
area, perimeter
convexity, convex perimeter
equivalent circle diameter
minimum, mean and maximum diameter
minimum, mean and maximum Feret diameter
minimum, mean and maximum Martin radius
minimum, mean and maximum enclosing rectangle area
x and y projection
shape factor, sphericity, elongation, aspect ratio of bounding rectangle
basic gray level derived
gray level variance, SD, min, max, kurtosis, skewness
integrated intensity
central moments derived
$\phi1$, $\phi2$, $\phi3$, $\phi4$, $\phi5$, $\phi6$, $\phi7$
GLCM derived
maximum, SD, mean, energy, contrast, homogeneity, entropy
Laws matrix energy
(for each matrix E5E5, E5R5, E5L5, L5E5, L5R5, L5L5, R5E5, R5R5, R5L5)

TABLE 2
Selected geometric features of the nuclei of the cases under study. RCC stands for renal cell carcinoma, PChRCC for probable chromophobe renal cell carcinoma. SD is standard deviation.

	area		mean diameter		shape factor		elongation	
chromophobe RCC	42.7	(SD 19.79)	7.7	(SD 1.81)	0.9	(SD 0.06)	1.3	(SD 0.27)
oncocytoma	34.2	(SD 11.37)	6.8	(SD 1.16)	1.0	(SD 0.04)	1.2	(SD 0.2)
clear cell RCC	39.2	(SD 21.15)	7.4	(SD 2.13)	0.9	(SD 0.08)	1.4	(SD 0.37)
PChRCC	39.0	(SD 19.81)	7.3	(SD 1.94)	0.9	(SD 0.07)	1.3	(SD 0.4)
all cases	40.2	(SD 19.82)	7.5	(SD 1.91)	0.9	(SD 0.07)	1.3	(SD 0.32)

performed with the KNN and EM algorithms, and the neural network method. All statistical analyses were performed with STATISTICA version 7.1. (StatSoft Inc, USA) and Excel 2003 (Microsoft Corp. USA). The significance level was set to 0.05.

Results

The material included 74 cases: 58 chromophobe carcinomas (ChRCC) and 16 oncocytomas (RO). For comparison, we included 54 cases of clear cell carcinoma (CCRCC) and 13 cases resembling chromophobe carcinoma, but not fulfilling all the classification criteria (probable chromophobe renal cell carcinoma, PChRCC). The average age of the patients was 61.9 years (SD 13.41), in the ChRCC group - 60.1, in the RO group - 59.0, in the CCRCC group - 63.9 and in the PChRCC group - 65.2. These differences are not statistically significant. In total, there were 62 females and 79 males, in the ChRCC group there were 29 females and 29 males, in the RO group - 11 females and 5 males, in the CCRCC group - 19 females and 35 males, and in the PChRCC group - 3 females and 10 males.

The average diameter of the tumor was 6.9 cm (SD 3.53), in the ChRCC group - 7.7cm, in the RO group - 6.7, in the CCRCC group - 6.6 and in the PChRCC group - 5.5 cm. These differences are not statistically significant.

Some geometric features of the nuclei are shown in Table 2 and Fig. 1. On ANOVA, there were statistically significant differences in all the parameters measured. In post-hoc analysis, ChRCC and RO showed differences in all the parameters; of the tumor types examined, only PChRCC showed lack of difference from other groups in some of the parameters examined.

It is noteworthy that nuclear features of ChRCC and RO are different, with significant ANOVA tests for all but very few parameters. However, a large degree of overlapping exists. When examining feature space on scatterplots (Fig. 2), this overlapping is particularly evident. With the dataset of this type, classification of the elements is particularly difficult. In the present investigations, neither the unsupervised KNN-based classification nor any of the used neural network classifiers was able to separate ChRCC and RO nuclei.

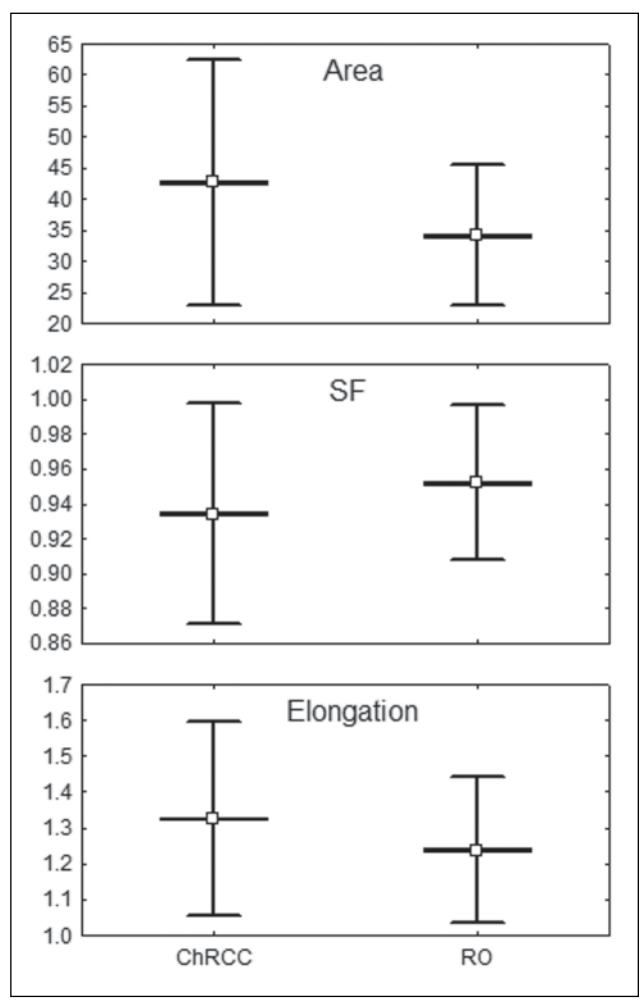

Fig 1. Comparison of the basic nuclear geometric features of chromophobe carcinoma (ChRCC) and oncocytoma (RO). The values are mean (central point), standard error (box) and standard deviation (whisker). SF is shape factor.

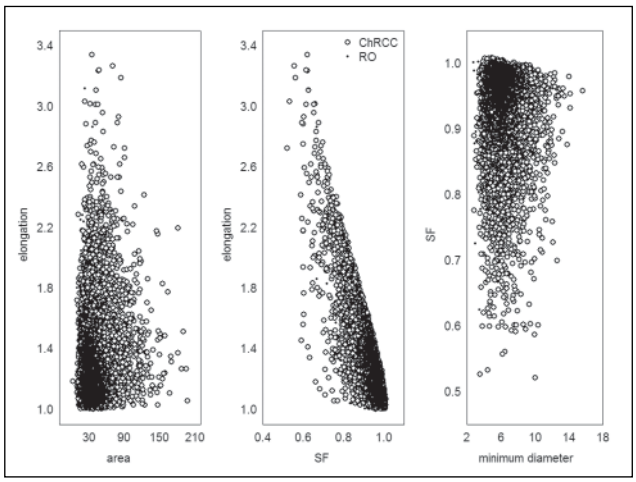

Fig 2. Scatterplots of nuclear features of chromophobe carcinoma (ChRCC, empty points) and oncocytoma (RO, small points). Left panel: elongation (y axis) versus area (x axis), central panel: elongation (y axis) versus shape factor (x axis), right panel: shape factor (y axis) versus minimum diameter (x axis).

Discussion

In some cases morphologic distinction between variants of ChRCC, ClearRCC and oncocytoma may be extremely difficult [24]. As these entities have different survival rates [2], this is of prime clinical importance. For this purpose, morphologic, ultrastructural, immunohistochemical and molecular methods may be used. Abrahams et al. [1] analyzed histological and immunohistological features of 32 tumors with uncertain features. Electron microscopy served as the gold standard. Based on light microscopy alone, the rate of agreement between experts was low (kappa=0.3). The features deemed most characteristic for ChRCC were accentuated cell borders and hyperchromatic, irregular nuclei surrounded by clear halos. The authors claim that the best immunohistochemical marker is parvoalbumin with 100% specificity and sensitivity exceeding 90%. Useful, but less effective were EMA, CD10 and CK7. Antimitochondrial antibody was also of some use. Hale's colloid iron and RCC antigen IHCh were not contributory in this series. In fact, the most classic feature of ChRCC is diffuse Hale's colloid iron reactivity [6]. However, Mai et al. [10] showed that a similar pattern of staining may be seen in several benign and malignant renal tumors, including ClearRCC, PapRCC and oncocytoma, rendering it less useful. ChRCC and tumors of intermediate histology, similar in some features to oncocytoma, are particularly frequent in Birt-Hogg-Dube syndrome. Among 130 renal tumors from 30 patients, Pavlovich et al. [16] found 44 ChRCC and 65 tumors with features of both ChRCC and oncocytoma. Skinnider et al. [22] studied the usefulness of cytokeratin immunohistochemistry in differential diagnosis of renal tumors. The phenotype of ChRCC in their study was CK7+, CK8+, CK18+, VIM-, and differed from that of oncocytoma mainly in CK7 negative staining in the later. Mazal et al. [12] found that expression of newly described "kidney specific" cadherin is highly restricted to chromophobe RCC and may be used as its diagnostic feature. In ChRCC it was positive in over 97%, but seen in 3% of oncocytomas and even less clear cell, papillary and collecting duct carcinomas. In this study CK7 was found to be also useful, but to a much lower extent. Mathers et al. [11] think that for differentiating oncocytoma from ChRCC CK7 immunohistochemistry is a good tool. Particularly, they stressed the reaction pattern as a distinguishing feature. For ChRCC, a strong cytoplasmic submembranous pattern is characteristic (100% of cases in this study), almost all conventional RCC were negative, and the only positive case, as well the oncocytomas show a weak, diffuse cytoplasmic reaction. This characteristic pattern of ChRCC was seen also in our study. According to Avery et al. [3], CD10 may be of some use for ChRCC differential diagnosis. All the cases in their study were negative, whereas a vast majority of ClearRCC and PapRCC were positive. However, this marker, as well as RCC antigen, does not add to differentiation between oncocytoma and ChRCC, as both of them are negative in most cases.

Young et al. [25] analyzed cDNA from various types of renal tumors with microarray technology. They found significant differences in expression of beta defensin 1, parvalbumin and vimentin and proposed to use these markers for immunohistochemical differential diagnosis. However, they found similar patterns in RO and ChRCC. Carrion et al. [4] showed that renal oncocytomas express caveolin-1 significantly stronger than RCCs and proposed to use this marker for differential diagnosis. Li et al. [8] analyzed ploidy pattern in different renal tumors by flow cytometry. They have seen diploid patterns in oncocytomas, but various non-diploid ones in ChRCC. In the later, hypodiploid cell population was present in some cases. No such population was seen in ClearRCC or PapRCC.

Castren et al. [5] were able to distinguish RCCs from renal oncocytomas using nuclear morphometry with very basic geometric features. In their work, shape parameters were the most discriminating features. They used a control RCC group matching the sex, age and size of specific oncocytoma cases. These results are quite interesting, but do not address the more recent RCC classification. Based on their data analysis, they believe that measuring 80 nuclei is sufficient for estimating the nuclear size.

References

1. *Abrahams NA, MacLennan GT, Khoury JD, Ormsby AH et al:* Chromophobe renal cell carcinoma: a comparative study of histological, immunohistochemical and ultrastructural features using high throughput tissue microarray. Histopathology 2004, 45, 593-602.
2. *Amin MB, Amin MB, Tamboli P, Javidan J et al:* Prognostic impact of histologic subtyping of adult renal epithelial neoplasms: an experience of 405 cases. Am J Surg Pathol 2002, 26, 281-291.
3. *Avery AK, Beckstead J, Renshaw AA, Corless CL:* Use of antibodies to RCC and CD10 in the differential diagnosis of renal neoplasms. Am J Surg Pathol 2000, 24, 203-210.
4. *Carrion R, Morgan BE, Tannenbaum M, Salup R et al:* Caveolin expression in adult renal tumors. Urol Oncol 2003, 21, 191-196.
5. *Castren JP, Kuopio T, Nurmi MJ, Collan YU:* Nuclear morphometry in differential diagnosis of renal oncocytoma and renal cell carcinoma. J Urol 1995, 154, 1302-1306.
6. *Eble JN, Sauter G, Epstein JI:* Tumours of the kidney. In: Eble JN, Sauter G, Epstein JI Ed: WHO Classification of Tumours: Pathology and Genetics of Tumours of the Urinary System and Male Genital Organs (World Health Organization Classification of Tumours). International Agency for Research on Cancer 2004, 9-88.
7. *Fleming S:* The impact of genetics on the classification of renal carcinoma. Histopathology 1993, 22, 89-92.
8. *Li G, Cottier M, Sabido O, Gentil-Perret A et al:* Different DNA ploidy patterns for the differentiation of common subtypes of renal tumors. Cell Oncol 2005, 27, 51-56.
9. *Linehan WM, Vasselli J, Srinivasan R, Walther MM et al:* Genetic basis of cancer of the kidney: disease-specific approaches to therapy. Clin Cancer Res 2004, 10, 6282S-9S.
10. *Mai KT, Burns BF:* Chromophobe cell carcinoma and renal cell neoplasms with mucin-like changes. Acta Histochem 2000, 102, 103-113.
11. *Mathers ME, Pollock AM, Marsh C, O'Donnell M:* Cytokeratin 7: a useful adjunct in the diagnosis of chromophobe renal cell carcinoma. Histopathology 2002, 40, 563-567.
12. *Mazal PR, Exner M, Haitel A, Krieger S et al:* Expression of kidney-specific cadherin distinguishes chromophobe renal cell carcinoma from renal oncocytoma. Hum Pathol 2005, 36, 22-28.
13. *Myler HR, Weeks AR:* The pocket handbook of image processing algorithms in c. Prentice Hall PTR, Eglewood Cliffs, New Jersey 1993.
14. *Okon K, Tomaszewska R, Nowak K, Stachura J:* Application of neural networks to the classification of pancreatic intraductal proliferative lesions. Anal Cell Pathol 2001, 23, 129-136.
15. *Parker JR:* Algorithms for image processing and computer vision. John Wiley & Sons Inc., New York, Chichester, Brisbane, Toronto, Singapore, Weinheim 1997.
16. *Pavlovich CP, Walther MM, Eyler RA, Hewitt SM et al:* Renal tumors in the Birt-Hogg-Dube syndrome. Am J Surg Pathol 2002, 26, 1542-1552.
17. *Renshaw AA:* Subclassification of renal cell neoplasms: an update for the practising pathologist. Histopathology 2002, 41, 283-300.
18. *Reuter VE:* The pathology of renal epithelial neoplasms. Semin Oncol 2006, 33, 534-543.
19. *Ries LAG, Harkins D, Krapcho M Eds:* SEER Cancer Statistics Review. 1975–2003. Bethesda, MD: National Cancer Institute; 2006. http://seer.cancer.gov/csr/1975_2003. 2006.
20. *Schalkoff RJ:* Digital image processing and computer vision. John Wiley & Sons Inc, New York, Chichester, Brisbane, Toronto, Singapore, Weinheim 1989.
21. *Schalkoff RJ:* Image analysis, part I. In: Schalkoff RJ Ed.: Digital image processing and computer vision. John Wiley & Sons Inc, New York, Chichester, Brisbane, Toronto, Singapore, Weinheim 1989, 254-332.
22. *Skinnider BF, Folpe AL, Hennigar RA, Lim SD et al:* Distribution of cytokeratins and vimentin in adult renal neoplasms and normal renal tissue: potential utility of a cytokeratin antibody panel in the differential diagnosis of renal tumors. Am J Surg Pathol 2005, 29, 747-754.
23. *Soft-Imaging Software:* Analysis imaging c. Soft-Imaging Software GmbH, Münster, Germany 1996.
24. *Thoenes W, Störkel S, Rumpelt HJ, Moll R et al:* Chromophobe cell renal carcinoma and its variants--a report on 32 cases.. J Pathol 1988, 155, 277-287.
25. *Young AN, de Oliveira Salles PG, Lim SD, Cohen C et al:* Beta defensin-1, parvalbumin, and vimentin: a panel of diagnostic immunohistochemical markers for renal tumors derived from gene expression profiling studies using cDNA microarrays. Am J Surg Pathol 2003, 27, 199-205.

Address for correspondence and reprint requests to:
Dr K. Okoń
Department of Pathomorphology Collegium Medicum,
Jagiellonian University
ul. Grzegórzecka 16
31-531 Kraków

ERRATUM:

Krzysztof Okoń[1], Agnieszka Klimkowska[1], Anna Pawelec[1], Zygmunt Dobrowolski[2], Zbigniew Kohla[3], Jerzy Stachura[1]

Immunophenotype and Cytogenetics of Mucinous Tubular and Spindle Cell Carcinoma of the Kidney

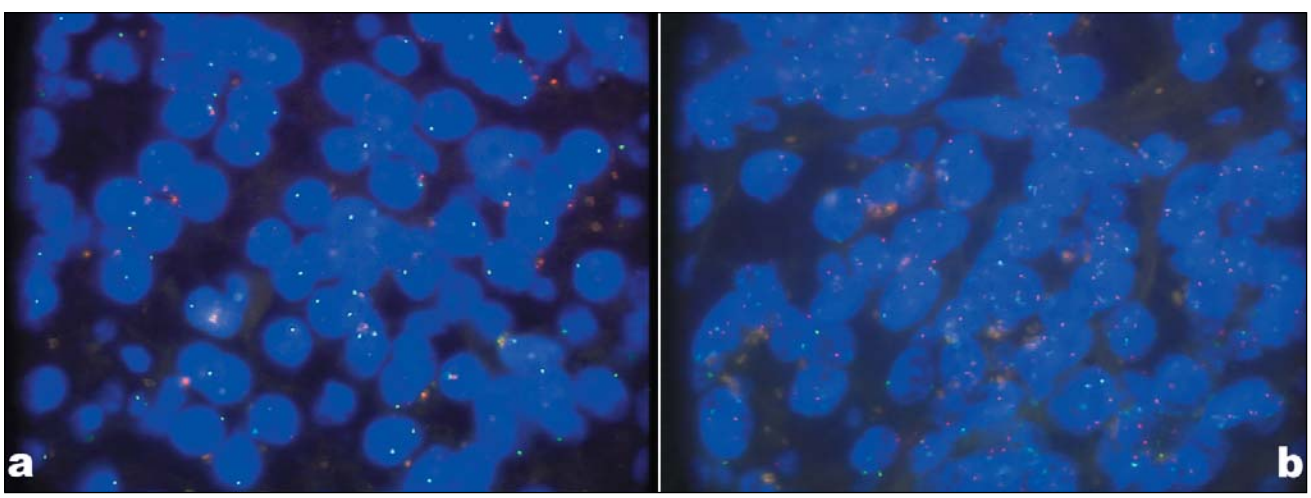

Fig. 5. Case 2, FISH results. a) chromosome 1 (red) & 8 (green) probes. Several cells contain single signals only. b) chromosome 7 (green) & 17 (red) probes. Additional signals in some of the cells. Lens magnification 100x.